Modelling the vibro-acoustic behaviour of expansion chamber silencers for fluid-filled pipe systems

Steven De Candia*, Stephen Moore, Ian MacGillivray and Alexei Skvortsov

Maritime Division, Defence Science and Technology, 506 Lorimer St Fishermans Bend VIC 3207, Australia
*Corresponding author: Steven.DeCandia@dst.defence.gov.au

ABSTRACT

Silencers for exhausts, pipe systems, and ducts often include an expansion chamber, which causes an impedance change in the pipe and transmission loss across the silencer. In pipe systems conveying a dense fluid, the elasticity of the expansion chamber wall can be an important factor affecting the vibro-acoustic behaviour of the silencer. This paper describes analytical and finite-element modelling of a silencer conveying such a dense fluid. The analytical approach used a fluid-filled beam model to describe the propagation of plane waves in the fluid, the structural response of the pipe, and Poisson coupling between the fluid and the structure. The finite element model was developed with the ANSYS Mechanical solver to conduct a fully coupled fluid-structure modal and harmonic response analysis. Results demonstrated that the analytical model was sufficient for predicting the transmission loss below the cut-on of transverse modes in the fluid and circumferential modes in the pipe. A significant advantage of the finite element model was the ability to model an internal rubber lining and also to identify how out-of-plane motion of expansion chamber flanges contributed to the transmission loss of the silencer.

1 INTRODUCTION

A substantial amount of research has been applied to acoustic propagation in pipes and ducts because the behaviour is relevant in many engineering applications. Examples include exhaust noise from internal combustion engines (Munjal, 1987), heating ventilation and air-conditioning systems (Bies and Hansen, 1996, Reynolds and Bledsoe, 1990), and industrial processes transporting gas and liquid (Norton and Karczub, 2003, de Jong, 1994, Tijsseling, 1996, Wiggert and Tijsseling, 2001). Analysis of these systems down to the component level can be a time consuming process, and design changes to a single component may have repercussions on the whole system, for better or worse, that need to be considered and understood in the evaluation of the whole system performance. Therefore, there would be notable benefit if the component effects on the system could be rapidly assessed, or at the very least have their general behaviour understood.

The two main approaches to modelling the vibro-acoustic behaviour of pipe systems are simplified analytical models (Munjal, 1987, Wiggert and Tijsseling, 2001, Tijsseling, 1996) and finite element models (ANSYS Inc., 2019, Tsuji, Tsuchiya, and Kagawa, 2002). Analytical models, for example rigid pipes or fluid-filled beam models, offer relatively quick solutions for simplified representations of the pipe systems, and valuable insights into the physical behaviour can often be inferred from the governing equations. However, these models also require a reasonably high level of expertise to implement and solve the analytical equations. Alternatively, Finite Element (FE) models can resolve the vibro-acoustic behaviour of pipe systems, but there is a trade-off between the frequency range considered and computation time. It can also be challenging to identify the physical mechanisms that produce particular behaviour from a single set of results, which necessitates numerical experimentation and thus longer computation times.

The present study investigates analytical and finite-element modelling of a silencer conveying a dense fluid. There can be strong fluid-structure interaction in such systems and the aim of the study is to identify the mechanisms that affect the transmission loss of the silencer and to illustrate the advantages of each modelling approach. The following section describes the silencer considered; Sections 3 and 4 summarise the analytical

and finite-element models; results from each modelling approach are discussed in Section 5, and concluding remarks are given in Section 6.

2 SILENCER STRUCTURE

The silencer considered is shown in Figure 1 and consisted of a 150 mm internal diameter, 500 mm long pipe with 10 mm thick walls. The inlet and outlet pipes were both of 50 mm internal diameter and a 20 mm thick flange connected these to the expansion silencer at each end. The inlet and outlet pipes were assumed rigid to highlight the vibro-acoustic behaviour of the expansion chamber. A 10 mm thick rubber liner surrounded the inside of the expansion chamber and the silencer was filled with water. All structural degrees of freedom were fixed at the ends of the inlet and outlet pipes.

Five configurations were evaluated:

1. Rigid structure
2. Elastic structure with rigid flanges
3. Elastic structure with elastic flanges
4. Elastic structure with a rubber liner and rigid flanges
5. Elastic structure with a rubber liner and elastic flanges

Configurations 2 and 4 consider the flange components as rigid, which is an inherent assumption in the analytical models.

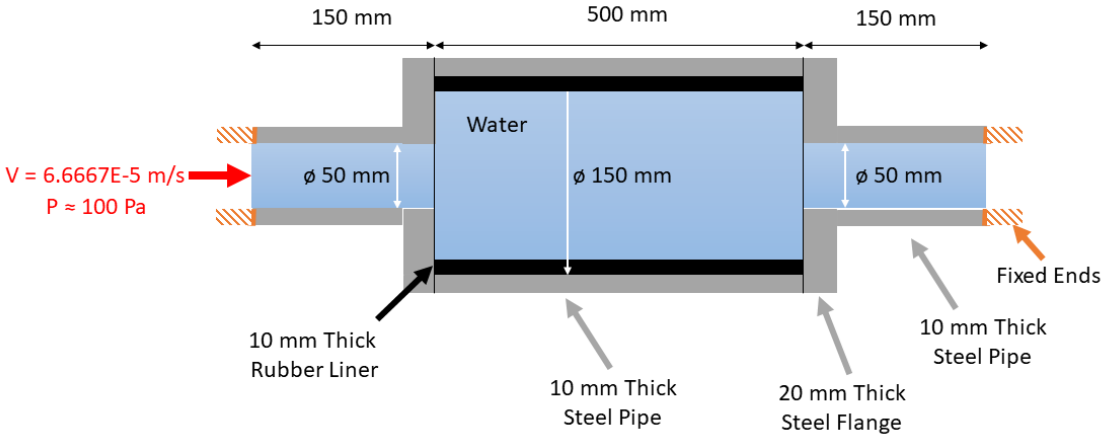

Figure 1 Expansion silencer

3 ANALYTICAL MODELS

Fluid loading on the pipe wall and the frequency range of interest influence the choice of analytical models for investigating acoustic propagation in pipes. One-dimensional plane wave models are appropriate for acoustic propagation in gases contained in pipes with relatively rigid walls (i.e. $K_f \ll E_s t/2a$; K_f is the fluid bulk modulus; a the mean pipe radius; E_s Young's modulus of pipe material; t pipe wall thickness). The plane wave assumption is accurate at frequencies below the cut-on frequency of transverse acoustic modes in the pipe (i.e. in round pipes $f < 0.5857 c_f/2a_i$ where c_f is the sound speed in the fluid, a_i is the pipe inner radius; and for square ducts $f < c_f/2h$ where h is the largest transverse dimension). In cases where fluid-loading is significant, wave propagation in the fluid and the pipe wall becomes coupled. In this scenario a fluid-filled beam model that accounts for axial, torsional, and bending deformation of the pipe, and one-dimensional plane wave propagation in the fluid can be adopted (Tentarelli, 1991, de Jong, 1994, Tijsseling, 1996, Kwong and Edge, 1996). This model is valid at relatively low frequencies and becomes inaccurate at frequencies above the cut-on frequency of transverse modes in the fluid and above the cut-on of lobar circumferential modes in the wall of circular cross-section pipes.

Both models (rigid-pipe and fluid-filled beam model) are implemented as transmission matrices and applied to illustrate the benefits of each approach.

3.1 Rigid Pipe Model

Plane wave propagation in a rigid pipe of constant cross-section is described by Equation (1) (Munjal, 1987), which relates the pressure and volume velocity at each end of the pipe. p_i and v_i are the pressure and volume velocity; S is the area of the pipe cross-section; ρ_f is the density of the fluid; c_f is the sound speed in the fluid; ω is the angular frequency; $k = \omega/c_f$ is the wavenumber; and l is the length of the pipe. The acoustic wave propagation along a system of pipes can be modelled by multiplying transmission matrices for each pipe section and setting boundary conditions at the inlet and outlet.

$$\begin{bmatrix} p_i \\ v_i \end{bmatrix} = \begin{bmatrix} \cos(kl) & j\frac{\rho_f c_f}{S}\sin(kl) \\ j\frac{S}{\rho_f c_f}\sin(kl) & \cos(kl) \end{bmatrix} \begin{bmatrix} p_{i+1} \\ v_{i+1} \end{bmatrix} \tag{1}$$

Figure 2 is a schematic of the expansion chamber silencer, which shows multiple pipe elements connected together. The inlet section of the pipe (between nodes 1 and 4) is split into three sections with identical cross-sectional areas to facilitate the calculation of the amplitude of the forward propagating wave. The expansion chamber presents an impedance change at nodes 4 and 5; and the outlet section of the pipe (between nodes 5 and 6) is terminated with an anechoic boundary condition; i.e. the terminating (load) impedance at node 6 equals the characteristic impedance of a plane wave in a pipe: $Z_6 = \rho_f c_f / S_5$.

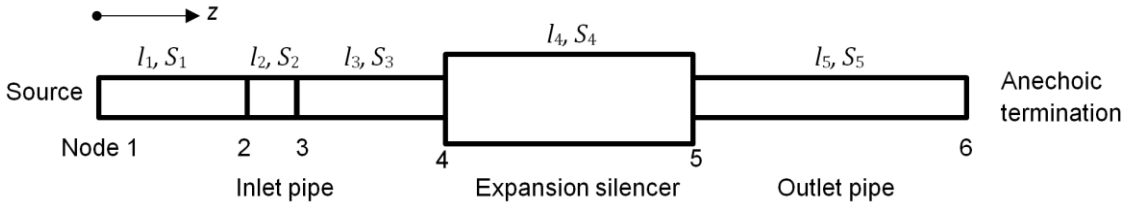

Figure 2 Schematic of expansion chamber silencer

The transmission loss of the arrangement of rigid pipes shown in Figure 2 is defined as the ratio of power incident on the silencer to the power transmitted by the silencer. The transmission loss can be calculated directly from the transmission matrix of the expansion chamber and the characteristic impedance at the inlet and outlet pipes ($\rho_f c_f / S$) (Munjal, 1987). An alternative approach that could be applied to both the rigid pipe model and also the fluid-filled beam model was adopted for the present study. The pressure at a point in a pipe is the sum of forward and backward propagating waves; i.e. $p = p^+ e^{-jkz} + p^- e^{jkz}$ (omitting the time dependence). The power of the incident wave is proportional to the forward propagating pressure wave in the inlet pipe, which can be determined from the pressure at two points, say nodes 2 and 3, using Equation (2).

$$p^+_{inlet} = (p_2 e^{jkz_3} - p_3 e^{jkz_2}) \frac{1}{2j\,\sin\big(k(z_3 - z_2)\big)} \tag{2}$$

The variables z_2 and z_3 are coordinates of the axial positions of the nodes relative to an arbitrary datum. Equation (2) is a function of wavenumber k, which in turn is dependent on the speed of sound of waves in the fluid. In rigid pipes this is determined only by the properties of the fluid and for elastic pipes discussed below, the speed of sound in the fluid is affected by the compliance of the pipe wall. The transmission loss is given by Equation (3), and it is emphasised that Equation (3) only applies to configurations with a non-reflecting termination at the outlet, and where the inlet and outlet internal dimensions are equivalent.

$$TL = 20\log\left(\frac{p^+_{inlet}}{p_{outlet}}\right) \tag{3}$$

3.2 Fluid-Filled Beam Model

The fluid-filled beam model is often referred to as the ‘fourteen equation model’ (Tijsseling, 1996). It describes the propagation of plane waves in the fluid, axial, torsional, bending and shear motion in the pipe, and

Poisson coupling between the fluid motion and axial motion of the pipe. The governing equations for the fluid-filled beam model are derived by a number of authors (Tentarelli, 1991, de Jong, 1994, Tijsseling, 2007), and a summary of the equations given by de Jong are reproduced in Table 1, with coordinates shown in Figure 3.

The axial motion of the fluid and the pipe is described by Equations (5) – (8); the Poisson coupling between fluid and structural motion by the $2\nu a/(E_s a_i S_s)$ coefficient of the last term in Equations (7) and (8). Flexural and torsional motion in the *x*-*z* plane is described by Equations (9) – (15) (similar equations apply to flexural motion in the *y*-*z* plane, after transposing coordinates). Equation (8) relates the gradient of fluid displacement (in the axial direction) to pressure and axial force (stress) in the pipe. The coefficient of the first term on the right-hand side of Equation (8) is the reciprocal of a modified bulk modulus of the fluid, and this accounts for the compliance of the pipe wall. The modified bulk modulus in Equation (8) and the fluid density (cf. Eq (5)) are used to define the effective sound speed of a pressure wave propagating in a fluid contained in an elastic pipe with free ends:

$$c_{eff} = \sqrt{\frac{1}{\rho_f \left[\left(\frac{1}{K_f} + \frac{2a}{t\,E_s}\right)\right]}} \tag{4}$$

Equation (4) suggests that the compliance of the pipe wall leads to the reduction of the effective sound speed in the fluid. This will also contribute to the impedance change that results from area discontinuities between the inlet, expansion chamber, and outlet pipes.

Table 1 Equations of motion (frequency domain) for a fluid-filled beam

Axial motion of pipe and fluid

$$\frac{\partial p}{\partial z} = \rho_f \omega^2 u_f \tag{5}$$

$$\frac{\partial F_z}{\partial z} = -\rho_s S_s \omega^2 u_z \tag{6}$$

$$\frac{\partial u_z}{\partial z} = \frac{F_z}{E_s S_s} - \frac{2\nu}{E_s}\frac{a}{a_i}\frac{S_f}{S_s}p \tag{7}$$

$$\frac{\partial u_f}{\partial z} = \left[-\frac{1}{K_f}\left(1 + \frac{2a}{t}\frac{K_f}{E_s}\right)\right]p + \frac{2\nu}{E_s}\frac{a}{a_i}\frac{F_z}{S_s} \tag{8}$$

Flexural motion of pipe (*x*-*z* plane)

$$\frac{\partial F_x}{\partial z} = -\left(\rho_s S_s + \rho_f S_f\right)\omega^2 u_x \tag{9}$$

$$\frac{\partial M_y}{\partial z} = -F_x - \rho_s I_s \omega^2 \varphi_y \tag{10}$$

$$\frac{\partial u_x}{\partial z} = \frac{F_x}{\kappa_s G_s S_s} + \varphi_y \tag{11}$$

$$\frac{\partial \varphi_y}{\partial z} = \frac{M_y}{E_s I_s} \tag{12}$$

Torsional motion

$$\frac{\partial M_z}{\partial z} = -\rho_s J_s \omega^2 \varphi_z \tag{13}$$

$$\frac{\partial \varphi_z}{\partial z} = \frac{M_z}{G_s J_s} \tag{14}$$

$$\kappa_s = \frac{2(1+\nu)}{(4+3\nu)} \tag{15}$$

$J_s \approx 2\pi^3 h$: torsional moment of inertia of pipe

a	mean pipe radius
a_i	internal pipe radius
K_f	bulk modulus of internal fluid
G_s	shear modulus of shell
I_s	area moment of inertia of pipe
κ_s	shear coefficient of thin walled pipe
S_s	cross-section area of pipe
S_f	cross-section area of fluid
ρ_s	density of pipe material
ν	Poisson's ratio of pipe material

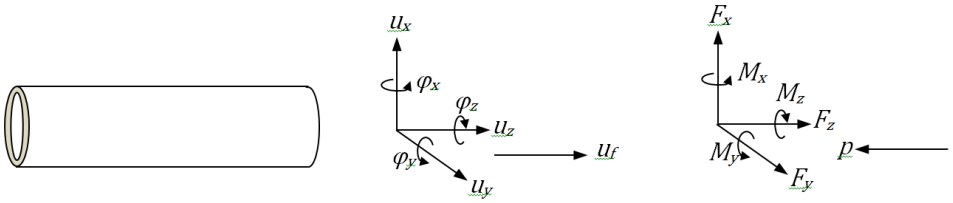

Figure 3 Coordinates and directions of displacements (u), rotations (φ), forces (F), moments (M), pressure (p) and fluid displacement (u_f) in a straight section of fluid-filled pipe.

The three sets of four coupled equations describing axial and flexural motion (Equations (5) – (12)) and the set of two coupled equations for torsional motion (Equations (13) – (14)) can be expressed as first-order differential equations of the form $\partial\mathbf{b}/\partial z = \mathbf{A}\mathbf{b}$, where $\mathbf{b}$ is a vector of state variables (e.g. $\mathbf{b} = \{p, F_z, u_f, u_z\}^T$) and $\mathbf{A}$ is a matrix of coefficients. Integrating the equation between two points yields a solution $\mathbf{b}|_2 = e^{\mathbf{A}(z_2 - z_1)}\mathbf{b}|_1$. The solutions for the four sets of equations are then assembled into a 14 x 14 transmission matrix relating the structural and fluid state variables at each end of the section of pipe; i.e. $\boldsymbol{x_i} = \{p, u_f, F_z, u_z, F_x, u_x, M_y, \varphi_y, F_y, u_y, M_x, \varphi_x, M_z, \varphi_z\}^T$. Further details are given by (de Jong, 1994, Kwong and Edge, 1996). The expansion chamber silencer is modelled by multiplying the transmission matrices for each section of pipe and applying boundary conditions. In this case a fluid volume velocity source was applied at the inlet and a non-reflecting boundary condition was applied to the fluid at the outlet. The pipe structural degrees-of-freedom at nodes 1 and 6 were fixed. The acoustic transmission loss was calculated using Equations 2 and 3 as described above.

4 FINITE ELEMENT MODEL

The FE model was developed and solved with the ANSYS Mechanical code (ANSYS Inc., 2019). The internal fluid volume was modelled with FLUID220 elements (3-D 20-node solid elements with quadratic pressure behaviour). The maximum element size was constrained by the frequency range of interest (0 – 2000 Hz), with a minimum of 6 elements per wavelength and calculated from $e_l = c_f/6f$; where e_l is element length; c_f is the sound speed in the fluid; and f is the maximum frequency of interest in Hz. It was also desirable to have at least 24 elements about the silencer circumference to capture the geometric curvature, which further reduced the maximum element size to approximately 0.02 m about the circumference. The casing and liner were constructed from SOLID186 elements, with a conformal mesh to the fluid domain. The mesh domains were coupled with shared nodes, which eliminated the need for contact elements. All elements used a quadratic shape function and were fully integrated.

Due to the small linear deformations, all structural elements used isotropic elastic properties, defined in Table 2. The steel properties were defined by Young's modulus and Poisson's ratio, while the rubber was defined by Young's modulus and bulk modulus. The additional properties were calculated by their relations automatically using ANSYS. Compressible behaviour was used in the fluid domain and the water was assigned density and acoustic velocity properties.

Table 2 Material properties used in finite element model

Property	Steel	Rubber	Water
Young's modulus (GPa)	200	6.3E-3	-
Bulk modulus (GPa)	167	2.4	-
Shear modulus (GPa)	77	2.1	-
Poisson's ratio	0.3	0.49956	-
Density (kg/m^3)	7850	950	1000
Acoustic velocity (m/s)	-	-	1500

The fluid and structural domains were fully coupled with an interface boundary condition that relates the node displacement $\{u_e\}$ and element pressure $\{p_e\}$ vectors at the interfaces of each domain. The governing equations are given in Equation (17), where $[M]$, $[C]$, and $[K]$ are the respective mass, damping, and stiffness matrices; $\{f\}$ is the excitation force vector; $\overline{\rho_0}$ is the acoustic fluid mass density constant; $[R]$ is the acoustic boundary matrix; and subscripts F and S denote the fluid and structure, respectively (ANSYS Inc., 2019).

$$\begin{Bmatrix} f_S \\ f_F \end{Bmatrix} = \begin{bmatrix} [M_S] & 0 \\ \overline{\rho_0}[R]^T & [M_F] \end{bmatrix} \begin{Bmatrix} \{\ddot{u}_e\} \\ \{\ddot{p}_e\} \end{Bmatrix} + \begin{bmatrix} [C_S] & 0 \\ 0 & [C_F] \end{bmatrix} \begin{Bmatrix} \{\dot{u}_e\} \\ \{\dot{p}_e\} \end{Bmatrix} + \begin{bmatrix} [K_S] & -[R] \\ 0 & [K_F] \end{bmatrix} \begin{Bmatrix} \{u_e\} \\ \{p_e\} \end{Bmatrix} \quad (17)$$

The inlet and outlet of the fluid domain were both assigned a non-reflecting radiation boundary condition, and a velocity amplitude of 6.6667E-5 m/s was applied to the fluid at the inlet cross-section. This equated to approximately 100 Pa assuming the characteristic impedance of a rigid inlet pipe. The harmonic analysis solution was run from 1 – 2000 Hz with a 1 Hz interval. Damping was applied only to the rubber liner material using a Material Dependant Damping model (ANSYS Inc., 2019) with a defined damping ratio of 3%.

5 MODEL COMPARISONS

The analytical and FE models were compared using the predicted transmission loss.

5.1 Rigid Structure

Transmission loss predicted for the rigid structure is shown in Figure 4 with very good agreement between the analytical rigid pipe and finite-element models. It can be shown using the rigid pipe analytical model that the minima in the transmission loss for simple expansion silencers correspond to the frequencies of multiples of half wave-lengths along the length of the expansion chamber (with adjustments to account for the finite impedance of the inlet and outlet pipes). That is $f_{minima} = nc_f/2L$, $n = 1,2,\ldots$, where L is the length of the expansion chamber. Figure 4 shows the first non-zero minimum in the transmission loss for the rigid silencer to be at 1507 Hz. Figure 5 shows the acoustic pressure at the frequency of the first maximum (752 Hz) and first non-zero minimum, and a half wavelength is evident along the length of the silencer at 1507 Hz. Note that the cut-on frequency of the first transverse acoustic mode in the pipe is approximately 5857 Hz; i.e. well above the analysis frequency range.

5.2 Elastic Structure

Due to the approximations in the fluid-filled beam model, two configurations of the elastic structure were considered: one in which the flanges were treated as rigid and one where they were elastic. The first configuration was a better representation of the analytical model, which didn't account for the radial offset of the pipe walls at junctions between the inlet pipe, expansion chamber, and outlet pipe. This meant that only the expansion chamber wall experienced elastic deformation, and the flanges of the silencer structure were treated as fixed boundary conditions. In the second configuration the elastic responses from both the silencer wall and flanges were coupled to the fluid domain.

5.2.1 Elastic Structure with Rigid Flanges

The fluid-filled beam model predicted the first non-zero minimum at 1387 Hz, which is consistent with the effective sound speed in the fluid of 1387.5 m/s calculated from Equation 4. Comparison of the analytical and FE results for the elastic structure with rigid flanges (Figure 4) shows excellent agreement with the first maximum (696 Hz) and minimum responses (1387 Hz), with a slightly larger variation in the level of transmission loss around the second maximum when compared to the rigid scenario. The acoustic pressure and structural displacements predicted by the finite-element model are shown in Figure 6, with quarter and half-acoustic wavelengths evident along the silencer at 696 Hz and 1387 Hz, respectively. The structural displacement is mostly driven by the pressure variation in the fluid.

Results in Figure 4 show that the maxima and minima in the transmission loss scale in frequency according to the effective sound speed in the fluid. The elastic expansion chamber also produces a slight increase the maximum transmission loss compared with the rigid pipe result, which is due to the increase in the impedance change between the expansion chamber and the connecting pipes.

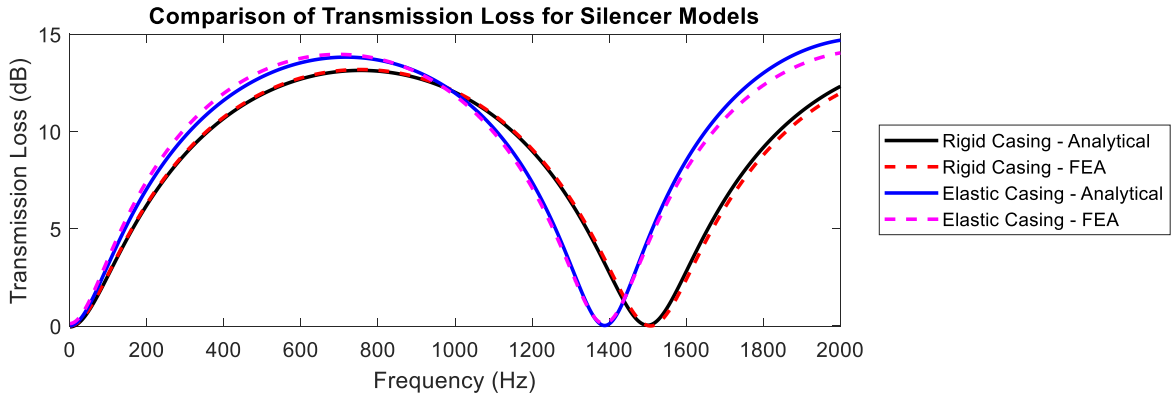

Figure 4 Transmission loss (TL) comparison between the analytical (solid) and FE models (dashed) for rigid and elastic structures.

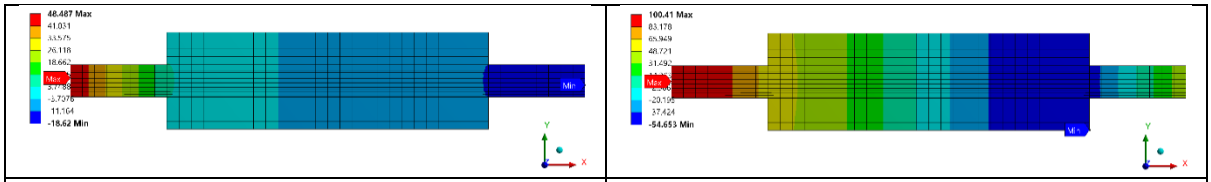

Pressure at TL maximum 1: 752 Hz	Pressure at TL minimum 1: 1507 Hz

Figure 5 Acoustic pressure predicted by the FE model for the rigid pipe silencer

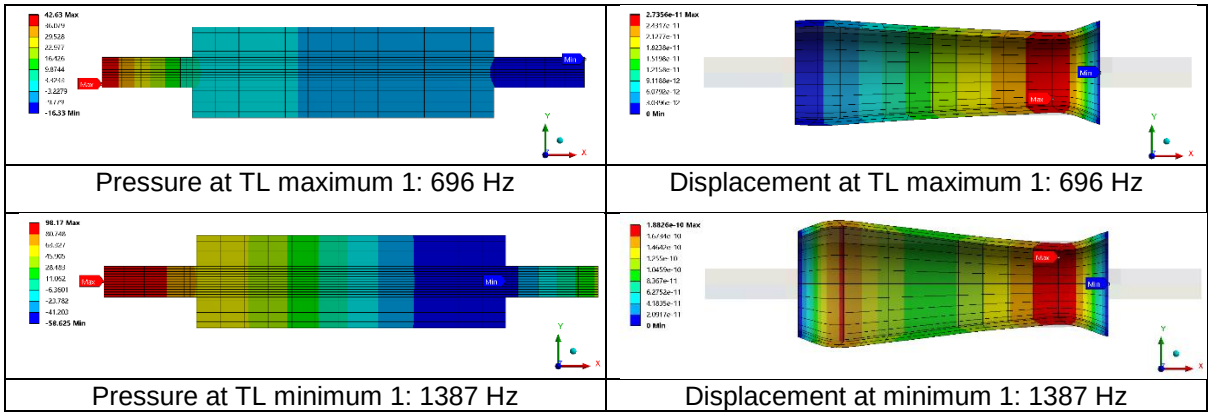

Pressure at TL maximum 1: 696 Hz	Displacement at TL maximum 1: 696 Hz
Pressure at TL minimum 1: 1387 Hz	Displacement at minimum 1: 1387 Hz

Figure 6 Acoustic pressure and (exaggerated) structural displacement for the elastic structure FE model with rigid flanges.

5.2.2 Elastic Structure with Elastic Flanges

With the introduction of elasticity in the flanges, the transmission loss below 800 Hz was still predicted well (Figure 7). Over 800 Hz the FE model presented a significant difference. There is a small shift in the first maximum from 696 Hz down to 640 Hz, while the first and second minima (1122 Hz and 1351 Hz) are separated by a second maximum at 1351 Hz, which has significant narrowband transmission loss. Structural displacement at frequencies corresponding to the maxima and minima of transmission loss (see Figure 8), show significant axial motion of the expansion chamber wall accompanied by out-of-plane bending of the end plates. This structural motion strongly couples to plane waves in the fluid and contributes to the increase in transmission loss. This illustrates the sensitivity of acoustic transmission loss to the structural response of the silencer and highlights a limitation of the analytical model; i.e. properly accounting for the structural dynamics

and fluid-structure coupling at pipe junctions with a change in cross-sectional area. However, there is still agreement between the analytical model and FE results up to approximately 640 Hz.

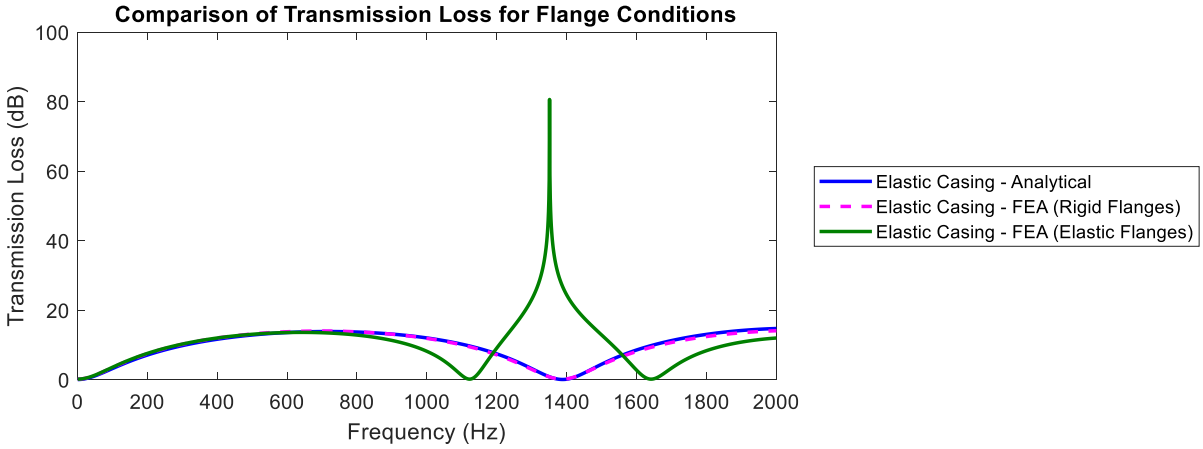

Figure 7 Transmission loss comparison for silencer structure with rigid and flexible flanges

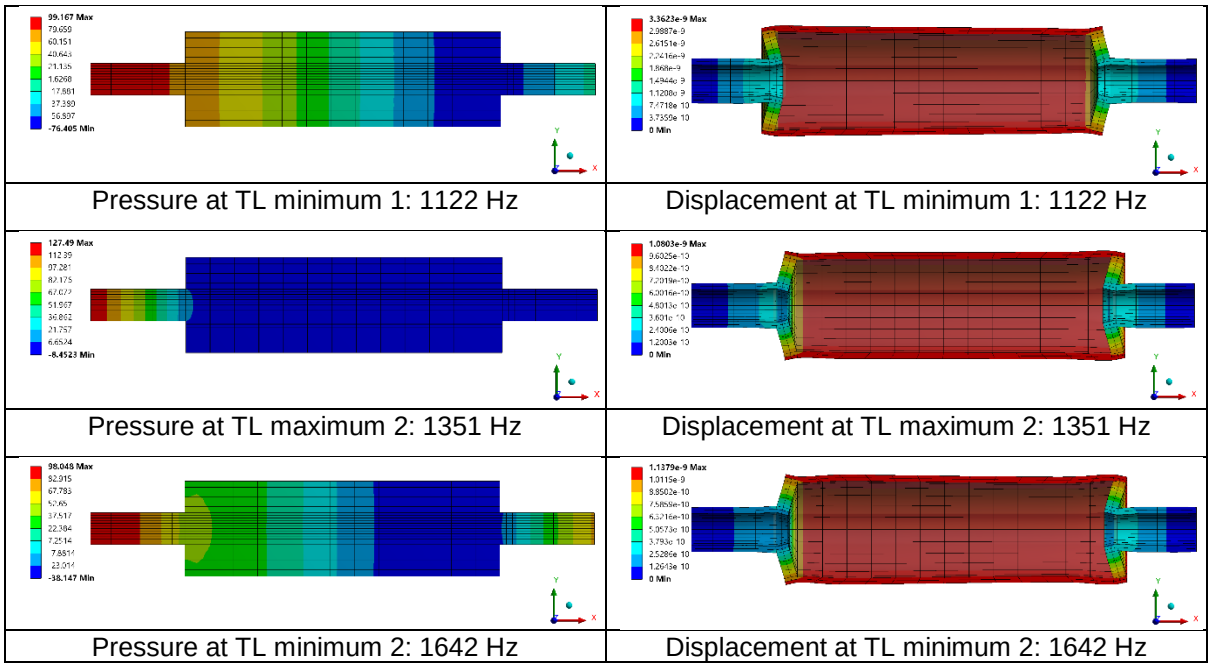

Figure 8 Acoustic pressure and (exaggerated) structural displacement for the elastic structure FE model with elastic flanges.

5.3 Elastic Structure with Rubber Liner

A rubber liner was introduced to the FE model, and as with the previous elastic structure comparisons, rigid and elastic flange configurations were considered. Transmission loss results for these configurations are compared to the previous un-lined configurations in Figure 9. These results show there was little difference in transmission loss at low frequencies up to the first maximum of the transmission loss for the lined configurations (approximately 575 Hz). At higher frequencies, the lined configurations begin to differ from the un-lined cases

5.3.1 Elastic Structure with Rubber Liner and Rigid Flanges

The first minimum occurred at 919 Hz for the elastic flange configuration and at 926 Hz for the rigid flange model. A second maximum was predicted for the rigid flange configuration at 1087 Hz. Structural displacement

results from the rigid flange configuration in Figure 10 show that at 1087 Hz (the second maximum) the performance is largely dominated by the response of the liner. The rigid flange also demonstrated a good broadband transmission loss between the first and second minimum; i.e. approximately 926 Hz – 1570 Hz.

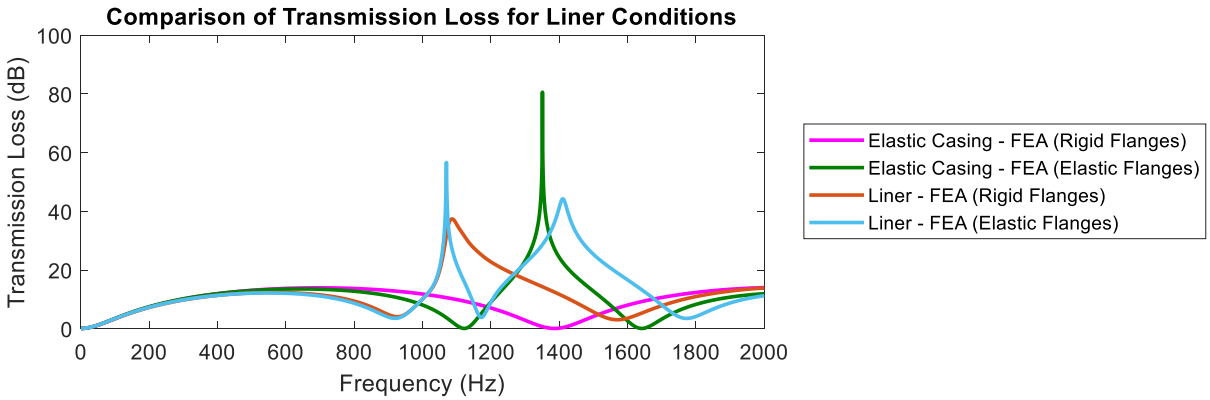

Figure 9 Transmission loss comparison for elastic structure FE models with rubber liner, rigid and elastic flange configurations.

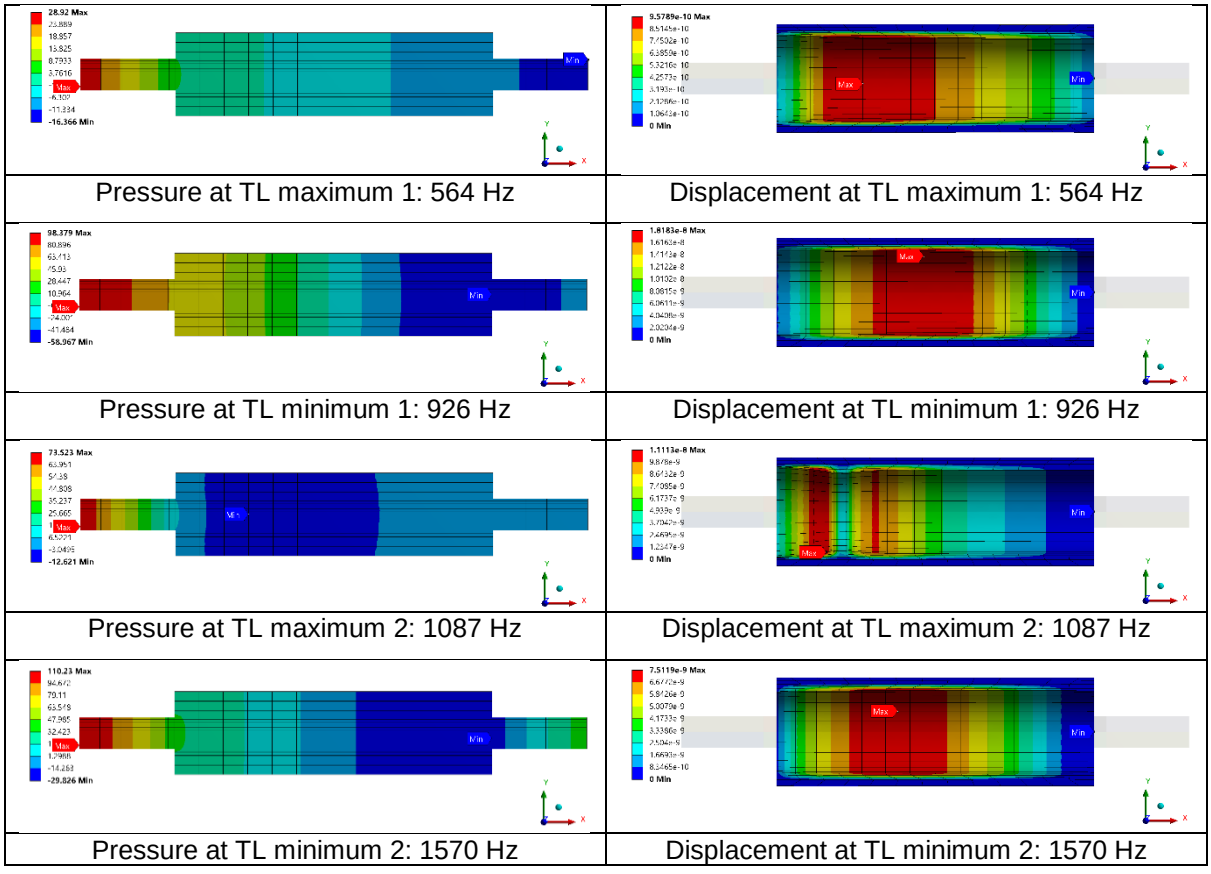

Figure 10 Acoustic pressure and (exaggerated) structural displacement for elastic structure FE model with rubber liner and rigid flanges.

5.3.2 Elastic Structure with Rubber Liner and Elastic Flanges

The elastic flange configuration transmission loss was nearly identical to the rigid flange configuration up to second maximum at 1070 Hz, although the narrowband transmission loss of the elastic flange model was much

greater at this maximum. The most significant difference for the lined elastic flange model was the presence of a second minimum, which occurred at 1172 Hz. Structural displacement results at 1172 Hz (Figure 11) show translational motion of the silencer pipe coupled with the liner response. A third maximum (1411 Hz) and minimum (1773 Hz) in the transmission loss were also new additions in the lined elastic flange model. From the structural displacements shown in Figure 11, it appears that the combined translational responses of the liner and silencer structures are responsible for the third maximum response (1411 Hz), but the third minimum response (1773 Hz) appears similar to the second minimum of the rigid flange model (1570 Hz; cf. Figure 10), where the liner motion dominates the response.

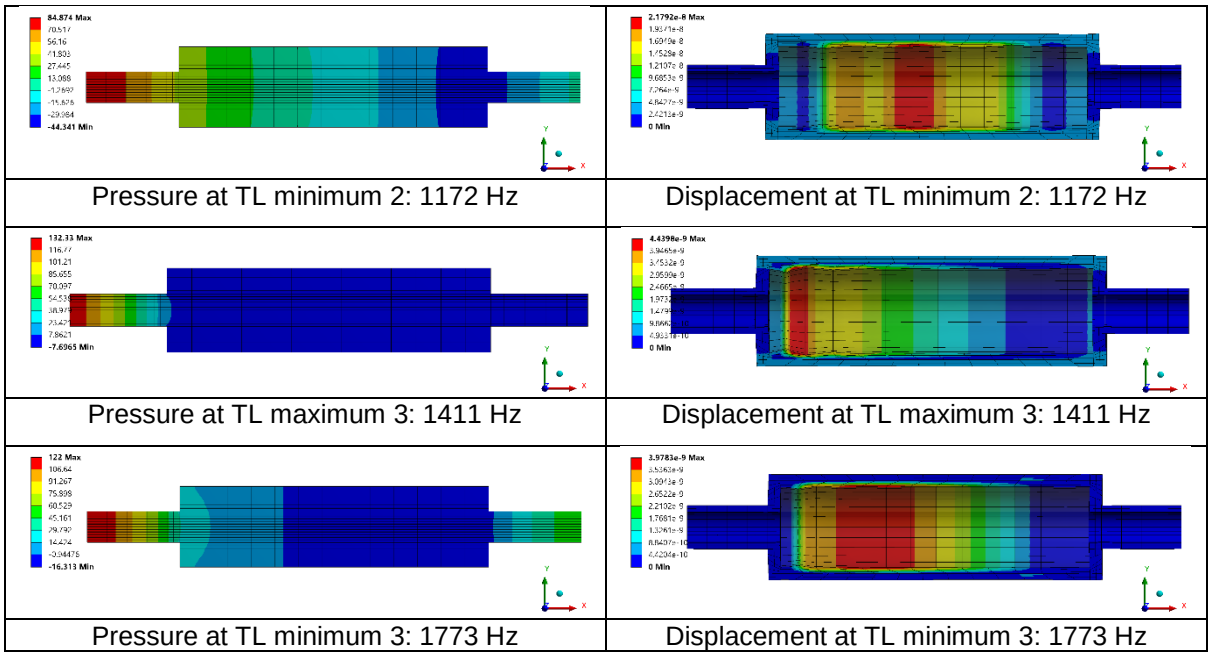

Pressure at TL minimum 2: 1172 Hz | Displacement at TL minimum 2: 1172 Hz

Pressure at TL maximum 3: 1411 Hz | Displacement at TL maximum 3: 1411 Hz

Pressure at TL minimum 3: 1773 Hz | Displacement at TL minimum 3: 1773 Hz

Figure 11 Acoustic pressure and (exaggerated) structural displacement for elastic structure FE model with rubber liner and elastic flanges.

6 CONCLUSION

An analytical model was developed to assess the acoustic performance of an expansion silencer structure, operating with a dense fluid. Comparison of predictions from this model to those from a finite element model showed excellent agreement for a completely rigid structure and for an elastic structure where the structural motion of flanges at area discontinuities was discounted. Out-of-plane motion of the flanges, which coupled to the plane waves in the fluid, was found to significantly affect the transmission loss, and the analytical model was unable to account for these effects. This resulted in significant variation in the predicted transmission loss between the analytical and finite element models at higher frequencies. Introduction of a rubber liner to the finite element model had a limited effect at low frequency but improved the high frequency performance above 1000 Hz. This was observed even if the translational motion of the flanges was neglected. In summary, these observations show that translational responses in a silencer structure can have significant effect on the performance and need to be considered for a reliable model that operates with a dense fluid.

REFERENCES

ANSYS Inc. 2019. *ANSYS 2019 R1 - Mechanical APDL Theory Manual*. Canonsburg, Pennsylvania: ANSYS Inc.

Bies, D.A., and C.H. Hansen. 1996. *Engineering Noise Control: Theory and Practice* 2nd ed. London: E. & F.N. Spon.

de Jong, C. 1994. "Analysis of pulsations and vibrations in fluid pipe systems."Ph.D. Thesis, TNO Institute of Applied Physics, Technische Universiteit Eindhoven.

Kwong, A., and K. Edge. 1996. 'Structure-borne noise prediction in liquid-conveying pipe systems'. *Proceedings of the Institution of Mechanical Engineers, Part I: Journal of Systems and Control Engineering* 210 (3):189-200.

Munjal, M.L. 1987. *Acoustics of ducts and mufflers with application to exhaust and ventilation system design*: John Wiley & Sons.

Norton, M.P., and D.G. Karczub. 2003. *Fundamentals of noise and vibration analysis for engineers*: Cambridge university press.

Reynolds, D.D., and J.M. Bledsoe. 1990. *Algorithms for HVAC Acoustic*. American Society of Heating, Refrigerating, and Air-Conditioning Engineers, Inc.

Tentarelli, S.C. 1991. 'Propagation of noise and vibration in complex hydraulic tubing systems'.

Tijsseling, A. 1996. 'Fluid-structure interaction in liquid-filled pipe systems: a review'. *Journal of Fluids and Structures* 10 (2):109-146.

Tijsseling, A. 2007. 'Water hammer with fluid–structure interaction in thick-walled pipes'. *Computers & structures* 85 (11-14):844-851.

Tsuji, T., T. Tsuchiya, and Y. Kagawa. 2002. 'Finite element and boundary element modelling for the acoustic wave transmission in mean flow medium'. *Journal of Sound and Vibration* 255 (5):849-866.

Wiggert, D.C., and A.S. Tijsseling. 2001. 'Fluid transients and fluid-structure interaction in flexible liquid-filled piping'. *Applied Mechanics Reviews* 54 (5):455-481.